Journal of Photochemistry and Photobiology A: Chemistry 217 (2011) 117–124

Contents lists available at ScienceDirect

Journal of Photochemistry and Photobiology A: Chemistry

journal homepage: www.elsevier.com/locate/jphotochem

Crystal structures and photoisomerization behaviors of five novel pyrazolone derivatives containing furoyl group

Jianping Hu, Lang Liu, Dianzeng Jia*, Jixi Guo, Xiangyun Xie, Dongling Wu, Rui Sheng

Institute of Applied Chemistry, Xinjiang University, Urumqi 830046, PR China

ARTICLE INFO

Article history:
Received 16 April 2010
Received in revised form 7 September 2010
Accepted 29 September 2010
Available online 7 October 2010

Keywords:
Photoisomerization
Crystal structure
Pyrazolone
Intermolecular proton transfer
Thiosemicarbazide

ABSTRACT

Five novel pyrazolone derivatives containing a furoyl group, 1-phenyl-3-furoyl-4-(4-chlorobenzal)-5-pyrazolone thiosemicarbazone (PF4ClBP-TSC) (**1**)/methylthiosemicarbazone (PF4ClBP-MTSC) (**2**)/ethylthiosemicarbazone (PF4ClBP-ETSC) (**3**), 1-phenyl-3-furoyl-4-(2-chlorobenzal)/(3-chlorobenzal)-5-pyrazolone methylthiosemicarbazone (PF2ClBP-MTSC) (**4**)/(PF3ClBP-MTSC) (**5**), have been synthesized and characterized by elemental analysis, IR, ^{1}H NMR spectra, and the molecular structures of **2** and **5** were determined by X-ray single crystal diffraction. Photoisomerization properties have been studied by UV–vis and fluorescence spectra. Based on theoretical calculation and crystal structural analysis, the compounds undergo photoisomerization from the enol form to the keto form through an intermolecular proton transfer upon UV light irradiation. Moreover, the photoisomerization rate decreases with the increase of volume of substituent groups on 4-position of thiosemicarbazide and the steric hindrance of Cl atom on benzal of 4-positon on the pyrazolone ring.

1. Introduction

Organic photochromic compounds have attracted considerable interest due to their promising applications in many fields, such as high-density optical storage media [1–3], molecular switches [4–8], information processors [9,10] and molecular sensors [11,12]. Considerable work on spiropyrans [13,14], spiroxazine [15–18], dithienylethenes [19,20], fulgides [21], and Schiff bases [22–25] have been extensively reported, but little work have been done on photochromism in solid state [26–28]. Most of organic photochromic compounds can only show photochromic properties in solution, however, these limit their application in solid state, such as ophthalmic plastic lenses, optical disks and digital versatile disks [29–31]. Recently, pyrazolones and their derivatives play important roles in many fields, especially biology, catalysis, corrosion inhibitors and medicine etc. [32–36]. Furthermore, 4-acyl pyrazolone derivatives have a potential to form tautomeric effect between the enol form and the keto form. So the molecular design and synthesis of novel pyrazolone derivatives is still an active research area. Many thiosemicarbazones derived from 4-acyl pyrazolones with photoisomerization properties have been systemically studied in our laboratory [37–41], but the majority show irreversible photoisomerization behaviors, thus many efforts have been dedicated to design the structures by changing the substitute groups on the 3- or 4-position on the pyrazolone ring and using other thiosemicarbazide derivatives. Previous works are focused on 1-phenyl-3-methyl or 1,3-diphenyl-4-acyl-5-pyrazolone thiosemicarbazone derivatives. For example, 1,3-diphenyl-4-(2-chlorobenzal)-5-hydroxypyrazole methylthiosemicarbazone [40], 1-phenyl-3-methyl-4-(2-fluorobenzal)-5-hydroxypyrazole methylthiosemicarbazone/ethylthiosemicarbazone [41], show a reversible photoisomerization. But these compounds display slow response to UV and visible light or incomplete reversibility. So their derivatives need to be further developed by the structural modification in order to improve the photochromic properties and establish the relation between structures and properties.

In this paper, five novel compounds, 1-phenyl-3-furoyl-4-(4-chlorobenzal)-5-pyrazolone thiosemicarbazone (**1**)/methylthiosemicarbazone (**2**)/ethylthiosemicarbazone (**3**), 1-phenyl-3-furoyl-4-(2-chlorobenzal)/(3-chlorobenzal)-5-pyrazolone methylthiosemicarbazone (**4**)/(**5**), are synthesized by the incorporation of the furoyl group on 3-position of pyrazolone. They are characterized by elemental analysis, IR, ^{1}H NMR spectra. With the aim of gaining a deeper insight into the photoisomerization mechanism, crystallographic structure analysis and theoretical calculation of the compounds have been carried out. The results show that the five compounds undergo photoisomerization from the enol form to the keto form through an intermolecular proton transfer upon UV light irradiation. In addition, the effects of volume of substituent groups on 4-position of thiosemicarbazide and the position of Cl atom on benzal on 4-position of pyrazolone ring on structures and photoisomerization properties of compounds were discussed

* Corresponding author. Fax: +86 991 8588883.
E-mail addresses: jdz0991@gmail.com, llyhs1973@sina.com (D. Jia).

1010-6030/$ – see front matter © 2010 Elsevier B.V. All rights reserved.
doi:10.1016/j.jphotochem.2010.09.027

in detail. These results will increase the knowledge to design and synthesize novel pyrazolone derivatives with photochromic properties in solid state.

2. Experimental

2.1. Measurements

Melting point was measured with a TECH X-6 melting point apparatus without correction. The C, H, and N elemental analysis was determined on a FLASHEA 1112 elemental analyzer. The FT-IR spectra were recorded on a BRUKER EQUINOX-55 Spectrometer as KBr disk. ^{1}H NMR spectra were carried at ambient temperature on an INOVA-400 NMR Spectrometer in DMSO-d_6. The UV–vis spectra of powders were measured using a Hitachi U-3010 spectrophotometer equipped with an integrating sphere accessory [36]. 365 nm excitation light (1579 mW/cm^2 on the sample) were down with a ZF-8 Ultraviolet Analysis Instrument, the reflective filter size is 200 × 80 mm, the distance between the sample and light source was 15 cm. Fluorescence spectra of powders were measured on a Hitachi F-4500 spectrophotometer with a front face experiment, and the breadths of excitation and emission slits were both 2.5 nm.

2.2. Materials

4-Methylthiosemicarbazide and 4-ethylthiosemicarbazide were purchased from the Aldrich Company, USA. 1-Phenyl-3-furoyl-5-pyrazolone (PFP) [42], 1-phenyl-3-furoyl-4-(4-chlorobenzal)-5-pyrazolone (PF4ClBP), 1-phenyl-3-furoyl-4-(2-chlorobenzal)-5-pyrazolone (PF2ClBP), and 1-phenyl-3-furoyl-4-(3-chlorobenzal)-5-pyrazolone (PF3ClBP) [43] were synthesized according to the literature. All other reagents were AR grade and purchased from commercial suppliers, and used without further purification.

2.3. Synthesis of compound *1*

1-Phenyl-3-furoyl-4-(4-chlorobenzal)-5-pyrazolone thiosemicarbazone was synthesized by refluxing of PF4ClBP (5 mmol) and thiosemicarbazide (5 mmol) in 15 ml of ethanol in the presence of glacial acetic acid (1 ml) at 80 °C for 4 h under magnetic stirring. Then the resulting mixture was cooled to room temperature in the dark and filtered, white powders **1** were obtained. Yield: 65.5%, m.p. 199.4–200.7 °C. Elemental analysis results for $C_{21}H_{16}N_5SO_2Cl$: found (%) C, 57.10; H, 3.67; N, 15.81; calcd. (%) C, 57.60; H, 3.68; N, 15.99. IR (ν cm^{-1}): (white) 3429 υ(NH), 3332, 3281 υ(NH), 3122 υ(furoyl), 3064–2000 υ(OH), 1612 υ(C=N), 1581–1501 υ(Ph-ring), 1413, 1374 υ(Pz-ring), 1302 υ(C=S). ^{1}H NMR (DMSO-*d*6) (δ): 9.728 (1H, NH), 8.301 (1H, NH), 8.479 (1H, NH), 6.321–7.876 (12H, phenyl + furoyl), 3.453(1H, CH).

2.4. Synthesis of compounds *2–5*

According to the synthetic method of **1**, compounds **2–5** were prepared. The synthesis routine and the photoisomerization process of five compounds are presented in Scheme 1. For yellowish powders **2**, yield: 84.5%, m.p. 227.3–229.1 °C. Elemental analysis results for $C_{22}H_{18}N_5SO_2Cl$: found (%) C, 57.94; H, 3.98; N, 15.52; calcd. (%) C, 58.47; H, 4.01; N, 15.50. IR (ν cm^{-1}): 3361, 3344 υ(NH), 3114 υ(furoyl), 3051–2215 υ(OH), 1622 υ(C=N), 1589–1501 υ(Ph-ring), 1417, 1375 υ(Pz-ring), 1305 υ(C=S). ^{1}H NMR (DMSO-*d*6) (δ): 9.756 (1H, NH), 8.795 (1H, NH), 6.328–7.873 (12H, phenyl + furoyl), 3.380 (1H, CH), 3.058–3.069 (3H, CH_3).

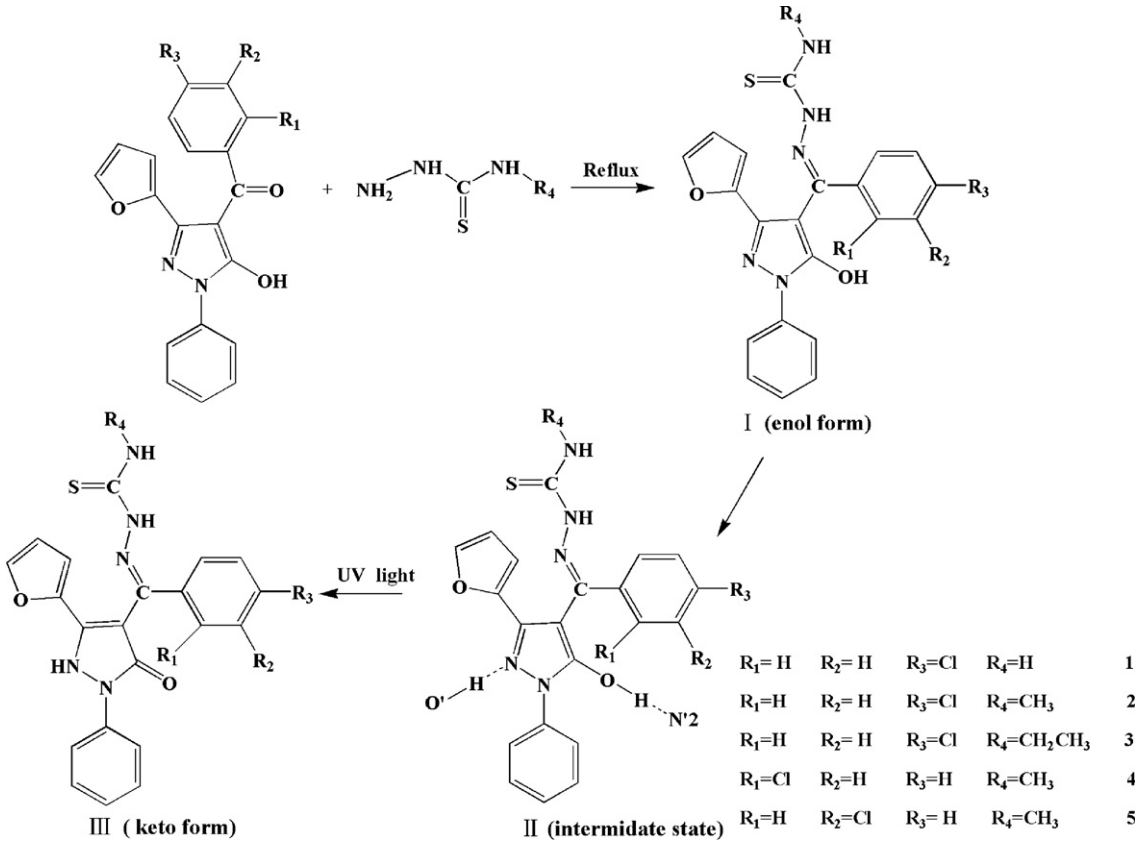

Scheme 1. Synthetic route and photoisomerization process of compounds.

For compound **3**, yield: 81.0%, m.p. 214.8–215.3 °C. Elemental analysis results for $C_{23}H_{20}N_5SO_2Cl$: found (%) C, 58.84; H, 4.30; N, 15.03; calcd. (%) C, 59.29; H, 4.33; N, 15.03. IR (ν cm^{-1}): 3331, 3311 υ(NH), 3121 υ(furoyl), 3069–2000 υ(OH), 1619 υ(C=N), 1579–1500 υ(Ph-ring), 1400, 1373 υ(Pz-ring), 1308 υ(C=S). ^{1}H NMR (DMSO-*d*6) (δ): 9.652 (1H, NH), 8.845 (1H, NH), 6.334–7.874 (12H, phenyl + furoyl), 3.618–3.650 (3H, CH_2 + CH), 1.159–1.195 (3H, CH_3).

For compound **4**, yield: 64.1%, m.p. 195.2–196.4 °C. Elemental analysis results for $C_{22}H_{18}N_5SO_2Cl$: found (%) C, 58.28; H, 4.12; N, 15.46; calcd. (%) C, 58.47; H, 4.01; N, 15.50. IR (ν cm^{-1}): 3351 υ(NH), 3116 υ(furoyl), 3054–2347 υ(OH), 1644 υ(C=N), 1594–1495 υ(Ph-ring), 1432, 1397 υ(Pz-ring), 1306 υ(C=S). ^{1}H NMR (DMSO-*d*6) (δ): 9.746 (1H, NH), 8.402 (1H, NH), 6.130–7.942 (12H, phenyl + furoyl), 2.921–3.038 (4H, CH + CH_3).

For compound **5**, yield: 76.8%, m.p. 214.8–216.4 °C. Elemental analysis results for $C_{22}H_{18}N_5SO_2Cl$: found (%) C, 58.27; H, 3.81; N, 15.31; calcd. (%) C, 58.47; H, 4.01; N, 15.50. IR (ν cm^{-1}): 3351, 3331 υ(NH), 3123 υ(furoyl), 3072–2000 υ(OH), 1520 υ(C=N), 1537–1480 υ(Ph-ring), 1416, 1373 υ(Pz-ring), 1307 υ(C=S). ^{1}H NMR (DMSO-*d*6) (δ): 9.849 (1H, NH), 8.813 (1H, NH), 6.324–8.015 (12H, phenyl + furoyl), 3.070–3.082 (4H, CH + CH_3).

2.5. X-ray crystallography

The X-ray diffraction data of compounds **2** and **5** were collected by the ω-scan mode using a graphite monochromatized Mo*Kα* radiation(λ = 0.71073 Å) on an imaging plate system (Rigaku R-AXIS SPIDER) at 296 K. Crystal structures were solved by direct methods and refined on F^2 using the full-matrix least-squares method. All non-H atoms were refined anisotropically. H atoms on nitrogen atoms are located from Fourier maps, and all of the other H atoms were placed in geometrically idealized position. All calculations and drawings were carried out using the SHELXTL-97 crystallographic software package [44].

3. Results and discussion

3.1. Photoisomerization properties in solid state and kinetics of the reaction

The UV spectra of five compounds in solid state at room temperature for different irradiation time intervals are recorded and shown in Fig. 1. It can be observed that new bands appear between 370 and 480 nm for **1**, 390 and 460 nm for **2**, 390 and 460 nm for **3**,

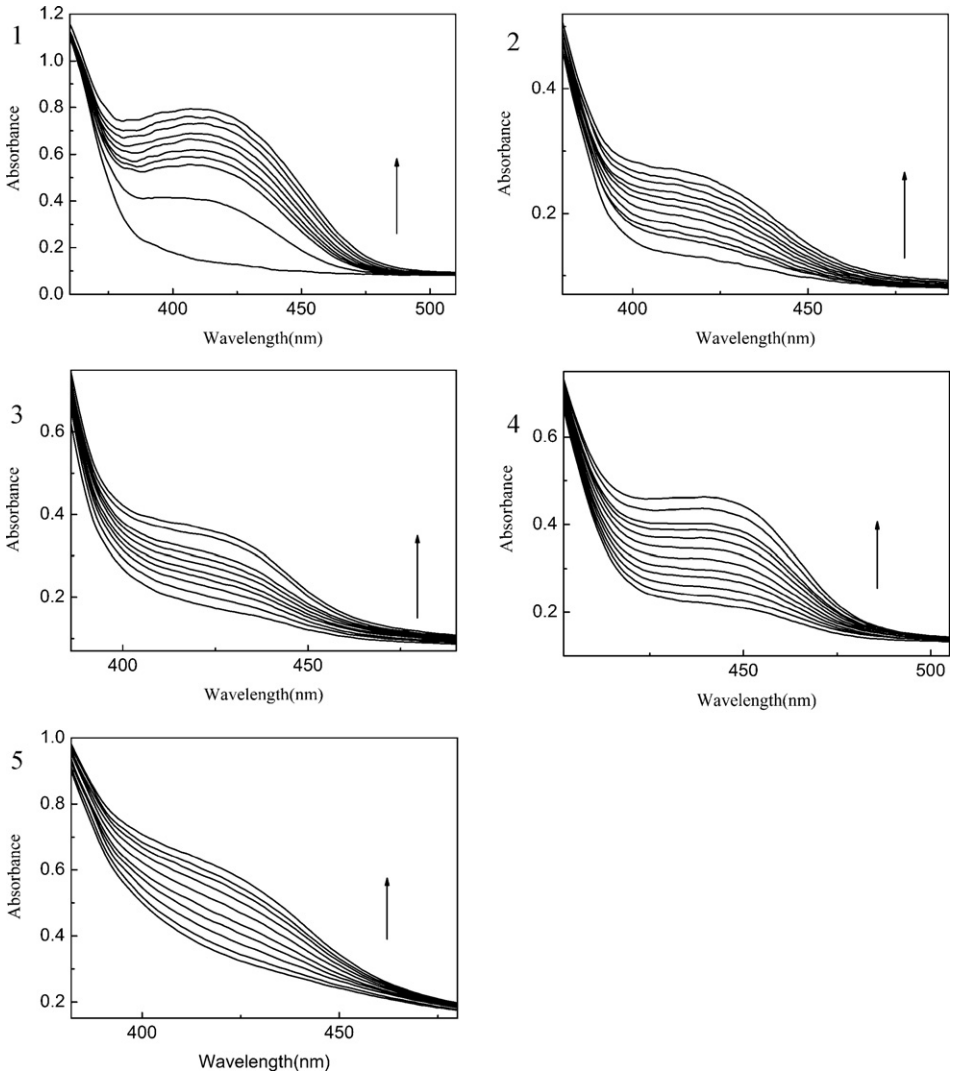

Fig. 1. UV spectra of five powders in the solid state with increasing irradiation times at room temperature. (1) Each irradiation time (min) for 1 is 0, 5, 15, 20, 25, 35, 45, 75, 105, 165. (2) Each irradiation time (min) for 2 is 0, 10, 20, 30, 50, 70, 110, 160, 200, 260, 330. (3) Each irradiation time (min) for 3 is 0, 30, 90, 150, 210, 290, 370, 450, 515, 650. (4) Each irradiation time (min) for 4 is 0, 10, 30, 60, 80, 100, 120, 140, 160, 180, 200, 220, 240, 280, 370, 500. (5) Each irradiation time (min) for 5 is 0, 30, 60, 100, 160, 220, 280, 330, 390, 420, 500.

410 and 480 nm for **4**, and 390 and 460 nm for **5** upon the irradiation of 365 nm light, and their intensities the increase of irradiation time. Subsequently, the white powders (I) changed to yellow (III) (Scheme 1). The results indicate that the photoisomerization from the enol form to the keto form occurs in solid state during the irradiation. No mater they are heated or irradiated by visible light or placed in the dark, the photogenerated yellow forms cannot return to the original forms, which indicate that the colored forms are very stable and the photoisomerization of five compounds is irreversible.

According to the literature [45], the kinetic rate constant can be determined from the plot of $\ln[(A_\infty - A_0)/(A_\infty - A_t)]$ against time (t). From Fig. 2, it can be observed that the enol-to-keto isomerization reaction of five compounds follow the pseudo-first-order kinetics and the rate constants were obtained from the slope. Obviously, the order of the photoisomerization rate of compounds **1**, **2** and **3** is $k_1 > k_2 > k_3$, which indicates that the photoisomerization rate decreases with the increase of volume of substituent groups on 4-position of thiosemicarbazide due to the larger steric hindrance. Compared with the photoisomerization rate constants of **4** and **5**, the photoisomerization rate of compound **2** is much faster than that of compounds **4** and **5**, which is due to the steric hindrance of Cl atom on the 4-position of the benzal is smaller than that of Cl on the 3-, 2-position of the phenyl group.

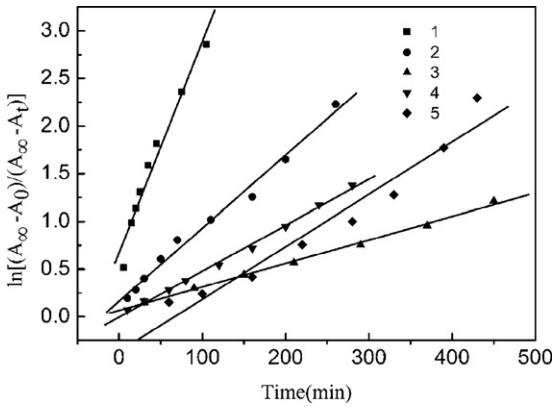

Fig. 2. First-order kinetic plot of photoisomerization reaction.

For the analogue compound 1,3-diphenyl-4-(2-chlorobenzal)-5-hydroxypyrazole 4-methylthiosemicarbazone, the kinetic con-

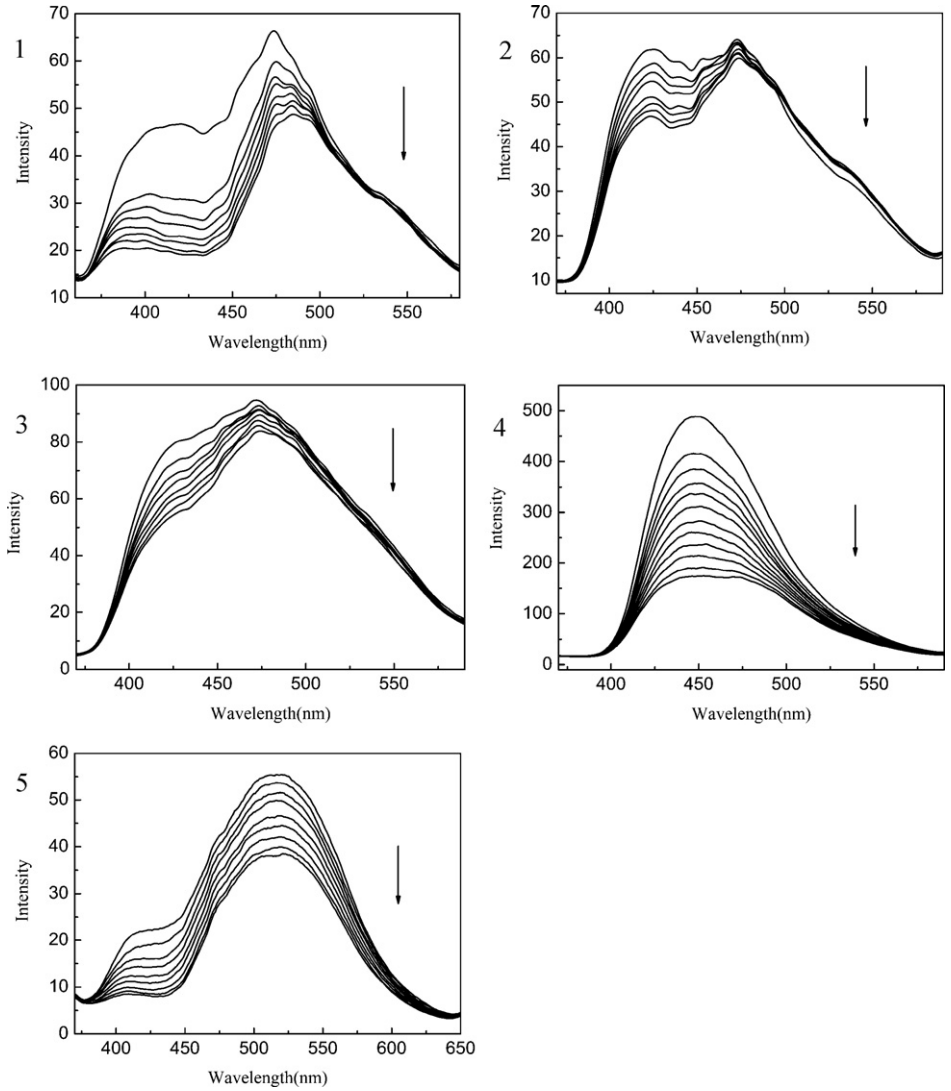

Fig. 3. Fluorescent emission spectra of five compounds under the irradiation of 365 nm UV light at room temperature (excited at 300 nm). (1) Each irradiation time (min) for 1 is 0, 0.5, 1, 3, 6, 12, 24, 51. (2) Each irradiation time (min) for 2 is 0, 2, 6, 12, 21, 30, 39, 48. (3) Each irradiation time (min) for 3 is 0, 1, 6, 12, 18, 27, 36, 42. (4) Each irradiation time (min) for 4 is 0, 0.5, 1, 2, 5, 11, 21, 31, 41, 56, 76, 96. (5) Each irradiation time (min) for 5 is 0, 3, 9, 15, 21, 27, 36, 45, 51.

Table 1
Absorption bands, kinetics constants and fluorescence maximum spectra of compounds.

Compounds	Absorption bands (nm)	Kinetics constants	Fluorescence maximum spectra
1	370–480	$3.69 \times 10^{-4}\ s^{-1}$	415 nm, 474 nm
2	390–460	$1.28 \times 10^{-4}\ s^{-1}$	425 nm, 474 nm
3	390–460	$4.1 \times 10^{-5}\ s^{-1}$	427 nm, 474 nm
4	410–480	$8.02 \times 10^{-5}\ s^{-1}$	448 nm
5	390–460	$9.17 \times 10^{-5}\ s^{-1}$	417 nm, 516 nm

stant of the photoisomerization is $1.72 \times 10^{-5}\ s^{-1}$, which is smaller than that of the compound **4**. The result shows that the photoisomerization rate of the compound **4** increases due to the electron withdrawing property of the O atom, when the furoyl group on 3-position of pyrazolone instead of the phenyl group.

The fluorescent emission spectra of five compounds irradiated by 365 nm UV light at different times at room temperature are shown in Fig. 3. It can be seen that there are two bands in the fluorescent emission spectra of **1**, **2** and **3**, which appear at 415 nm and 474 nm for **1**, 425 nm and 474 nm for **2**, 427 nm and 474 nm for **3**, respectively (Table 1), their intensity gradually decreased with the irradiation of 365 nm light. Furthermore, the second bands of three compounds lie in the same position, but the first bands have the red-shift phenomenon with the increase of volume of substituent groups on 4-position of thiosemicarbazide, which are consistent with those of their UV absorption spectra. Compared with the second band of **2**, the fluorescent emission spectra of **4** blue shifts to 448 nm and that of **5** red shifts to 516 nm after being excited at 300 nm, which is due to the steric hindrance of Cl atom on the 4-position of benzal. Obviously, their intensity gradually decreased with the irradiation of 365 nm light, and the emission band at 415 nm (**1**), 427 nm (**3**) and 417 nm (**5**) finally disappeared. Subsequently, the white enol form (I) gradually changed to the yellow keto form (III), the dramatic color changes can be explained by the photoinduced proton transfer from one moiety to another, the proton transfer and configuration rearrangement of the π electrons lead to fluorescent emission spectra changes in the solid state, which further indicate that five compounds have photoisomerization behaviors. However, UV light stationary irradiation has no influence on the absorption and fluorescence spectra of the different compounds in solution.

3.2. Crystal structure, stability and photoisomerization mechanism

Single crystals of compounds **2** and **5** were obtained by the slow evaporation of their methanol at room temperature with avoiding sunlight. The crystal data and structure refinement details of compounds **2** and **5** are given in Table 2. Selected bond lengths and bond angles are listed in Table 3. The dihedral angles (°) of two compounds are listed in Table 4. The molecular structures of compounds **2** and **5** are shown in Fig. 4.

From Table 2, it can be seen that compounds **2** and **5** have the same composition, but they have the different crystal system, space group and unit cell parameter. From Table 3, it can be found that the two compounds have similar bond length and bond angles, leading to similar structures as shown in Fig. 4. But obvious difference is the relative orientation of two groups (chlorophenyl and methylthiosemicarbazide) on the 4-position of the pyrazolone ring. From Table 4, it can be found that the dihedral angle of the pyrazole ring (I) and the furoyl ring(III) on 3-position is almost 1.4° for **2**, which indicates that the two planes are coplanar. In addition, the dihedral angles between the chlorophenyl(IV) and the plane(V) defined by N3, N4, N5, C21 atoms are 3.4° for **2** and 4.5° for **5**, respectively, which show that the side-chain groups for **2** and **5** are almost coplanar.

Table 2
Crystal data and structure refinement for compounds **2** and **5**.

Compounds	**2**	**5**
Empirical formula	$C_{22}H_{18}ClN_5O_2S$	$C_{22}H_{18}ClN_5O_2S$
Formula weight	451.92	451.92
Temperature	153(2) K	153(2) K
Wavelength	0.71073 Å	0.71073 Å
Crystal system	Orthorhombic	Monoclinic
Space group	*Pna*2(1)	*P*2(1)/*c*
Unit cell dimensions	$a = 11.771(2)$ Å, $\alpha = 90°$ $b = 11.916(2)$ Å, $\beta = 90°$ $c = 14.556(3)$ Å, $\gamma = 90°$	$a = 13.0250(8)$ Å, $\alpha = 90°$ $b = 14.4207(8)$ Å, $\beta = 104.490°$ $c = 11.6216(6)$ Å, $\gamma = 90°$
Volume	2041.9(7) Å^3	2113.4(2) Å^3
Z	4	4
Calculated density	1.470 g/cm^3	1.420 g/cm^3
Absorption coefficient	0.321 mm^{-1}	0.310 mm^{-1}
F(000)	936	936
Crystal size	0.50 × 0.35 × 0.23 mm	0.35 × 0.14 × 0.11 mm
Theta range for data collection	3.42–27.48°	3.06–27.48°
Limiting indices	$-15 \le h \le 15$, $-15 \le k \le 15$, $-18 \le l \le 18$	$-16 \le h \le 16$, $-18 \le k \le 18$, $-15 \le l \le 15$
Reflections collected/unique	18605/2430 [$R_{(int)} = 0.0237$]	20103/4843 [$R_{(int)} = 0.0434$]
Max. and min. transmission	0.9310 and 0.8556	0.9667 and 0.8993
Refinement method	Full-matrix least-squares on F^2	Full-matrix least-squares on F^2
Data/restraints/parameters	2430/4/292	4843/3/293
Goodness-of-fit on F^2	1.080	1.087
Final *R* indices [$I > 2\sigma(I)$]	$R_1 = 0.0266$, $wR_2 = 0.0686$	$R_1 = 0.0434$, $wR_2 = 0.1204$
R indices (all data)	$R_1 = 0.0270$, $wR_2 = 0.0689$	$R_1 = 0.0514$, $wR_2 = 0.1280$
Extinction coefficient	0.0059(8)	0.0063(12)
Largest diff. peak and hole	0.240 and −0.297 eÅ^{-3}	0.366 and −0.422 eÅ^{-3}

Table 3
Selected bond lengths (Å) and angles (°) for compounds **2** and **5**.

2		5	
Bond lengths			
S–C(21)	1.683(2)	S–C(21)	1.6811(2)
N(1)–N(2)	1.389(2)	N(1)–N(2)	1.3756(2)
N(1)–C(7)	1.378(2)	N(1)–C(7)	1.3845(2)
C(8)–C(9)	1.389(2)	C(8)–C(9)	1.391(2)
N(1)–C(6)	1.432(2)	N(1)–C(6)	1.427(2)
N(2)–C(9)	1.356(2)	N(2)–C(9)	1.345(2)
N(3)–C(14)	1.286(3)	N(3)–C(14)	1.290(2)
N(3)–N(4)	1.359(2)	N(3)–N(4)	1.3559(2)
N(4)–C(21)	1.365(3)	N(4)–C(21)	1.372(2)
N(5)–C(21)	1.324(3)	N(5)–C(21)	1.323(2)
O(1)–C(7)	1.253(2)	O(1)–C(7)	1.2548(2)
Bond angles			
N(2)–N(1)–C(6)	120.37(15)	N(2)–N(1)–C(6)	121.64(12)
C(9)–N(2)–N(1)	107.71(14)	C(9)–N(2)–N(1)	108.94(11)
C(7)–N(1)–N(2)	109.80(16)	C(7)–N(1)–N(2)	108.80(12)
N(3)–C(14)–C(8)	125.65(17)	N(3)–C(14)–C(8)	124.39(14)
N(1)–C(7)–C(8)	105.91(15)	N(1)–C(7)–C(8)	106.34(13)
N(2)–C(9)–C(8)	109.78(16)	N(2)–C(9)–C(8)	109.14(14)
N(5)–C(21)–N(4)	116.42(18)	N(5)–C(21)–N(4)	115.62(15)
N(5)–C(21)–S	124.99(16)	N(5)–C(21)–S	126.59(14)
N(4)–C(21)–S	118.59(15)	N(4)–C(21)–S	117.79(12)

Table 4
The dihedral angles (°) of two compounds.

	The mean plane deviation	Dihedral angles
2		
I (N1, N2, C7, C8, C9)	0.0139	
II (C1–C6)	0.0146	47.1
III (C10–C13, O2)	0.0036	1.4, 46.9
IV (C15–C20)	0.01	65.6, 34.8, 66.3
V (N3, N4, N5, C21)	0.0123	67.0, 33.5, 36.7, 3.4
5		
I (N1, N2, C7, C8, C9)	0.0091	
II (C1–C6)	0.0110	32.2
III (C10–C13, O2)	0.0009	8.5, 27.2
IV (C15–C20)	0.0059	76.2, 83.4, 73.7
V (N3, N4, N5, C21)	0.0391	70.6, 79.6, 67.3, 7.8

Table 5
Calculated electronic energies E (in a.u.), relative electronic energies ΔE (in kcal mol^{-1}), and dipole moment μ (in Debye) of compounds **2** and **5** in the gas phase and methanol solution.

	2	**5**
E^{gas}_{enol} (a.u.)	−2131.715360	−2131.711851
E^{gas}_{keto} (a.u.)	−2131.714540	−2131.714047
ΔE^{gas}_{keto}	0.52	−1.38
μ^{gas}_{enol}	3.6912	4.3981
μ^{gas}_{keto}	5.4892	4.4993
E^{sol}_{enol} (a.u.)	−2131.744713	−2131.744199
E^{sol}_{keto} (a.u.)	−2131.752006	−2131.751616
ΔE^{sol}_{enol}	−4.58	−4.66

However, the chlorophenyl and methylthiosemicarbazide will rotate around the C8–C14 bond when the position of Cl atom changes. As shown in Scheme 2, it is very clear that the relative orientation of chlorophenyl and methylthiosemicarbazide with the pyrazole ring are different due to the steric hindrance of Cl atom, leading to the dihedral angle between the pyrazole ring(I) and the phenyl ring(II) on 1-position is also different.

The C7–O1 bond distances are 1.253(2) Å for **2** and 1.2548(2) Å for **5**, respectively, which is consistent with the length of the C=O double bond. It can be deduced that their structures belong to the keto (III) form in Scheme 1, which is in agreement with the compounds reported previously [40,41]. Actually, we only obtained the keto form crystals from their solution. In order to further analyze the stability of the keto and enol forms, theoretical calculations are performed with the GAUSSIAN 03W program package [46]. The geometric parameters of the keto form are taken from the X-ray diffraction crystal data. The calculated electronic energies E, relative electronic energies ΔE, and dipole moment μ of compounds **2** and **5** in the gas phase and methanol solution are shown in Table 5. Although the enol form of **2** is more stable than the keto form in the gas phase, the keto form of **2** is the favored form in methanol solution, as the larger dipole moment μ of keto form (5.4892 Debye for keto, 3.6912 Debye for enol) [47,48] and a small energy gap of 0.52 kcal mol^{-1} between the two forms. On the con-

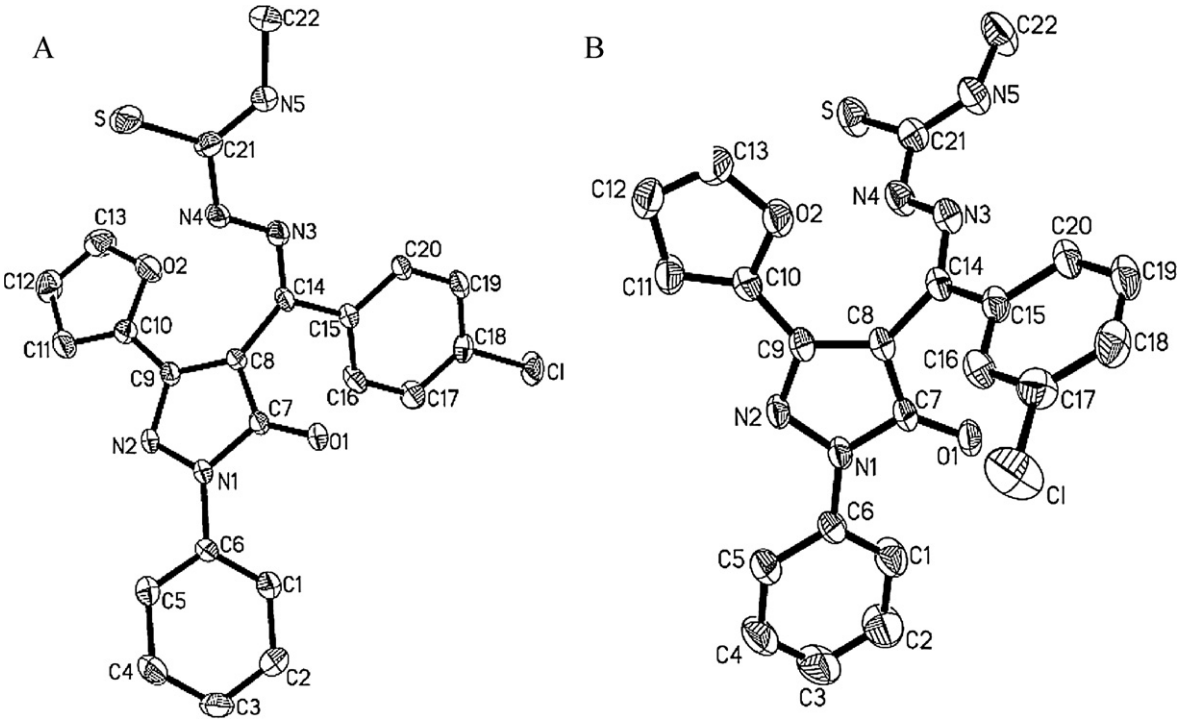

Fig. 4. Molecular structures of compound **2** (A) and **5** (B).

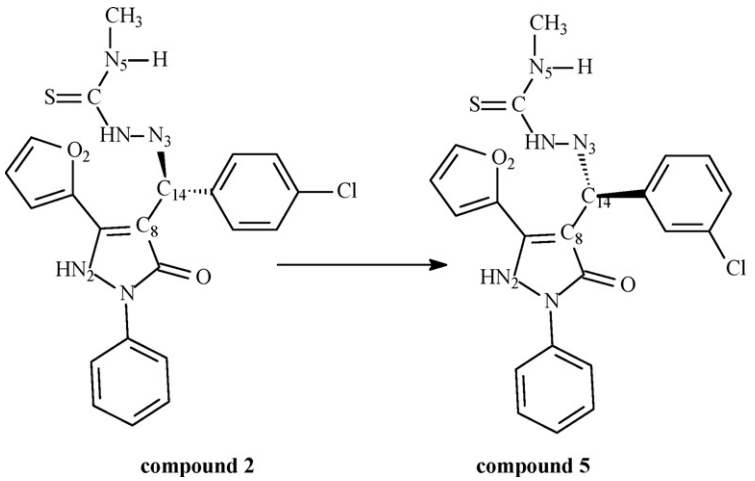

Scheme 2. Rotation of the chlorophenyl and methylthiosemicarbazide around the C_8–C_{14}.

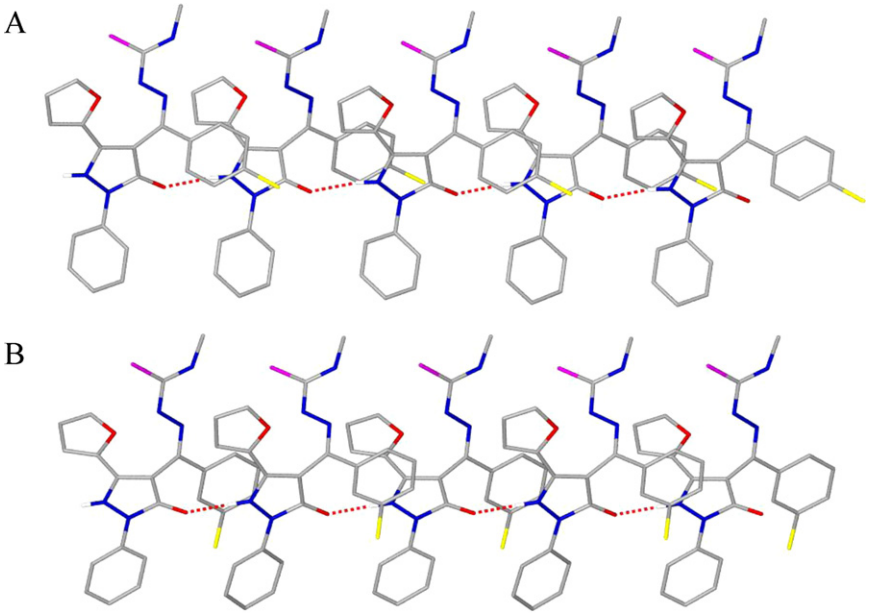

Fig. 5. Hydrogen bond connection diagrams of compounds **2** (A) and **5** (B).

trary, the keto form of **5** is predicted as the more stable form in the gas phase, and the order of stability is preserved in methanol solution because of the small difference of μ (μ^{gas}_{enol} = 4.3981 Debye, μ^{gas}_{keto} = 4.4993 Debye). The calculated results suggest that the keto form of **2** and **5** is the most stable isomer in methanol solution, which is in good agreement with the experimental fact that the single crystal structures of the compounds obtained from methanol are the keto forms [41].

From the hydrogen bond connection diagrams (Fig. 5), it can be seen that there is a similar hydrogen bonding configuration in the two crystals, and they are stabilized by the intermolecular hydrogen bond (N2–H···O1, 2.784 Å or 2.642 Å). Based on the above analysis, a reasonable photoisomerization mechanism is proposed. Under UV light irradiation, the intermolecular proton transfers from the O atom to the N2 atom by the channel of N2–H···O1, forming an intermolecular hydrogen bond N2–H···O1. Thus, it results in the enol–keto photoisomerization through the intermolecular hydrogen bond via the intermediated state (II) as shown in Scheme 1. The photoisomerization mechanism of the title compounds is consistent with that of 1-phenyl-3-methyl-4-(3-chlorobenzal)-5-hydroxypyrazole methylthiosemicarbazone [37], but is different from that of the analogous compound 1,3-diphenyl-4-(2-chlorobenzal)-5-hydroxypyrazole methylthiosemicarbazone, which is not only an intramolecular proton transfer from the O atom of the hydroxyl group to the N(4) atom of the same molecule, but also an intermolecular proton transfer from the S atom to the N(2) atom on pyrazole ring of the adjoining molecule [40]. These results indicate that substituent groups on 3-, 4-position have important effect on the structures and photochromic properties.

4. Conclusion

Five novel pyrazolone derivates containing a furoyl ring have been synthesized. Crystal structure analysis and theoretical calculation suggest the photoisomerization is the result of isomerization from the enol-form to the keto-form by the intermolecular proton transfer via hydrogen bond. After the furoyl group on 3-position of pyrazolone ring instead of the phenyl group, the photoisomerization rate decreases with the increase of volume of substituent groups on 4-position of thiosemicarbazide and the steric hindrance

of Cl atom on benzal of 4-positon of the pyrazolone ring. These results are useful for the design and synthesis of novel pyrazolone derivatives with photochromic properties in solid state.

Acknowledgements

This work was supported by the National Natural Science Foundation of China (No. 20762010), Program for New Century Excellent Talents in Universities of China (NCET-09-0904), The Key Project of Ministry of Education, China (209138), and the Natural Science Foundation of Xinjiang Uygur Autonomous Region (2009211B02).

Appendix A. Supplementary data

Supplementary data associated with this article can be found, in the online version, at doi:10.1016/j.jphotochem.2010.09.027.

References

[1] G.Y. Jiang, S. Wang, W.F. Yuan, Z. Zhao, A.J. Duan, C.M. Xu, L. Jiang, Y.L. Song, D.B. Zhu, Photo- and proton-dual-responsive fluorescence switch based on a bisthienylethene-bridged naphthalimide dimer and its application in security data storage, Eur. J. Org. Chem. (2007) 2064–2067.
[2] S.Z. Xiao, Y. Zou, M.X. Yu, T. Yi, Y.F. Zhou, F.Y. Li, C.H. Huang, A photochromic fluorescent switch in an organogel system with non-destructive readout ability, Chem. Commun. (2007) 4758–4760.
[3] G.Y. Jiang, S. Wang, W.F. Yuan, L. Jiang, Y.L. Song, H. Tian, D.B. Zhu, Highly fluorescent contrast for rewritable optical storage based on photochromic bisthienylethene-bridged naphthalimide dimer, Chem. Mater. 18 (2006) 235–237.
[4] F.L.E. Jakobsson, P. Msrsal, S. Braun, M. Fahlman, M. Berggren, J. Cornil, X. Crispin, Tuning the energy levels of photochromic diarylethene compounds for opto-electronic switch devices, J. Phys. Chem. C 113 (2009) 18396–18405.
[5] C.W. Lee, Y.H. Song, Y. Lee, K.S. Ryu, K.W. Chi, Reversible photochromic switch ensemble and its photoimaging using H^+ transfer between spiropyran and fluorescein in a polymer matrix, Chem. Commun. (2009) 6282–6284.
[6] Z.X. Li, L.Y. Liao, W. Sun, C.H. Xu, C. Zhang, C.J. Fang, C.H. Yan, Reconfigurable cascade circuit in a photo- and chemical-switchable fluorescent diarylethene derivative, J. Phys. Chem. C 112 (2008) 5190–5196.
[7] M. Tomasulo, S. Sortino, F. Raymo, Bichromophoric photochromes based on the opening and closing of a single oxazine ring, J. Org. Chem. 73 (2008) 118–126.
[8] N.V. Mockus, D. Rabinovich, J.L. Petersen, J.J. Rack (Eds.), Femtosecond isomerization in a photochromic molecular switch, Angew. Chem. Int. 47 (2008) 1458–1461.
[9] J. Andrasson, S.D. Straight, S. Bandyopadhyay, R.H. Mitchell, T.A. Moore, A.L. Moore, D. Gust, A molecule-based 1:2 digital demultiplexer, J. Phys. Chem. C 111 (2007) 14274–14278.
[10] J. Andre#asson, S.K. Straight, T.A. Moore, A.L. Moore, D. Gust, Molecular all-photonic encoderdecoder, J. Am. Chem. Soc. 130 (2008) 11122–11128.
[11] V.A. Krongauz, C.P. Bosnjak, A. Chudnovsky, Use of photochromic spiropyran as a molecular probe of large strain in polycarbonate, High Energy Chem. 43 (2009) 454–460.
[12] V. Lemieux, N.R. Branda, Reactivity-gated photochromism of 1,2-dithienylethenes for potential use in dosimetry applications, Org. Lett. 7 (2005) 2969–2972.
[13] J.R. Chen, D.Y. Yang, Design and synthesis of an *o*-hydroxyphenyl-containing spiropyran thermochromic colorant, Org. Lett. 11 (2009) 1769–1772.
[14] X.F. Guo, D.Q. Zhang, G.X. Zhang, D.B. Zhu, Molecular logic: "Half-Adder" based on multistate/multifunctional photochromic spiropyrans, J. Phys. Chem. B 108 (2004) 11942–11945.
[15] Z.B. Zhang, C.R. Zhang, M.G. Fan, W.P. Yan, Synthesis and complexation mechanism of europium ion (Eu^{3+}) with spiro[indoline-phenanthrolineoxazine], Dyes Pigments 77 (2008) 469–473.
[16] M.R. di Nunzio, P.L. Gentili, A. Romani, G. Favaro, Photochromic, thermochromic, and fluorescent spirooxazines and naphthopyrans: a spectrokinetic and thermodynamic study, ChemPhysChem 9 (2008) 768–775.
[17] M Suzuki, T. Asahi, H. Masuhara, Temperature dependence of ultrafast photoinduced ring-opening and -closure reactions of spironaphthooxazine in crystalline phase, J. Photochem. Photobiol. A: Chem. 178 (2006) 170–176.
[18] M. Suzuki, T. Asahi, K. Takahashi, H. Masuhara, Ultrafast dynamics of photoinduced ring-opening and the subsequent ring-closure reactions of spirooxazines in crystalline state, Chem. Phys. Lett. 368 (2003) 384–392.
[19] M. Akazawa, K. Uchida, J.J.D. de Jong, J. Areephong, M. Stuart, G. Caroli, W.R. Browne, B.L. Feringa, Photoresponsive dithienylethene-urea-based organogels with "reversed" behavior, Org. Biomol. Chem. 6 (2008) 1544–1547.
[20] R.H. Mitchell, S. Bandyopadhyay, Linked photoswitches where both photochromes open and close, Org. Lett. 6 (2004) 1729–1732.
[21] Y. Ishibashi, M. Murakami, H. Miyasaka, S. Kobatake, M. Irie, Y. Yokoyama, Laser multiphoton- gated photochromic reaction of a fulgide derivative, J. Phys. Chem. C 111 (2007) 2730–2737.
[22] M. Ziólek, J. Kubicki, A. Maciejewski, R. Naskrecki, A. Grabowska, Enol-keto tautomerism of aromatic photochromic Schiff base *N,N′*-bis(salicylidene)-*p*-phenylenediamine: ground state equilibrium and excited state deactivation studied by solvatochromic measurements on ultrafast time scale, J. Chem. Phys. 124 (2006), 124518-1–124518-10.
[23] Z. Liang, Z.L. Liu, Y.H. Gao, Synthesis, characterization and photochromic studies of three novel calyx[4]arene-Schiff base, Spectrochim. Acta A 68 (2007) 1231–1235.
[24] M. Sliwa, N. Mouton, C. Ruckebush, S. Aloïse, O. Poizat, G. Buntinx, R. Métivier, K. Nakatani, H. Masuhara, T. Asahi, Comparative investigation of ultrafast photoinduced processed in salicylidene-aminopyridine in solution and solid state, J. Phys. Chem. C 113 (2009) 11959–11968.
[25] M. Sliwa, A. Spangenberg, I. Malfant, P.G. Lacroix, R. Métivier, R.B. Pansu, K. Nakatani, Structural, optical, and theoretical studies of a thermochromic organic crystal with reversibly variable second harmonic generation, Chem. Mater. 20 (2008) 4062–4068.
[26] F. Robert, A.D. Naik, B. Tinant, R. Robiette, Y. Garcia, Insights into the origin of solid-state photochromism and thermochromism of n-salicylideneanils: the intriguing case of aminopyridines, Chem. Eur. J. 15 (2009) 4327–4342.
[27] N.S.S. Kumar, S. Varghese, C.H. Suresh, N.P. Rath, S. Das, Correlation between solid-state photophysical properties and molecular packing in a series of indane-1,3-dione containing butadiene derivatives, J. Phys. Chem. C 113 (2009) 11927–11935.
[28] L. Liu, X.Y. Xie, D.Z. Jia, J.X. Guo, X.L. Xie, Synthesis and properties of a novel photochromic compound with modulated fluorescence in the solid state, J. Org. Chem. 75 (2010) 4742–4747.
[29] J.C. Crano, R.J. Guglielmetti, Organic Photochromic and Thermochromic Compounds, Plenum Press, New York, 1999.
[30] Q.F. Luo, H. Tian, B.Z. Chen, W. Huang, Effective non-destructive readout of photochromic bisthienylethene–phthalocyanine hybrid, Dyes Pigments 73 (2007) 118–120.
[31] V.A. Barachevsky, Photonics of organic photochromic systems: modern trends, J. Photochem. Photobiol. A: Chem. 196 (2008) 180–189.
[32] T. Yoshikuni, Cerium complexes with phthaloylbis(pyrazolone) ligands as an efficient catalysts for cresols dioxygenation, J. Mol. Catal. A: Chem. 148 (1999) 285–288.
[33] A. Kimata, H. Nakagawa, R. Ohyama, T. Fukuuchi, S. Ohta, T. Suzuki, N. Miyata, New series of antiprion compounds: pyrazolone derivatives have the potent activity of inhibiting protease-resistant prion protein accumulation, J. Med. Chem. 50 (2007) 5053–5056.
[34] M.F. Braña, A. Gradillas, A.G. Ovalles, B. López, N. Acero, F. Llinares, D.M. Mingarro, Synthesis and biological activity of *N,N*-dialkylaminoalkyl-substituted bisindolyl and diphenyl pyrazolone derivatives, Bioorg. Med. Chem. 14 (2006) 9–16.
[35] D. Costa, A.P. Marques, R.L. Reis, J.L.F.C. Lima, E. Femandes, Inhibition of human neutrophil oxidative burst by pyrazolone derivatives, Free Radic. Biol. Med. 40 (2006) 632–640.
[36] A.S. Fouda, A.A. Al-Sarawy, E.E. El-Katori, Pyrazolone derivatives as corrosion inhibitors for C-steel in hydrochloric acid solution, Desalination 201 (2006) 1–13.
[37] J.X. Guo, L. Liu, D.Z. Jia, J.H. Wang, X.L. Xie, Solid-state photochromic properties and mechanism of 1-phenyl-3-methyl-4-(3-chlorobenzal)-5-hydroxypyrazole 4-methylthiosemicarbazone, J. Phys. Chem. A 113 (2009) 1255–1258.
[38] L. Liu, D.Z. Jia, Y.L. Ji, K.B. Yu, Synthesis, structure and photochromic properties of 4-acyl pyrazolone derivants, J. Photochem. Photobiol. A: Chem. 154 (2003) 117–122.
[39] T. Zhang, G.F. Liu, L. Liu, D.Z. Jia, L. Zhang, Solid-state proton transfer studies on phototautomerization of 1-phenyl-3-methyl-4-furoyl-5-pyrazolone 4-methyl thiosemicarbazone, Chem. Phys. Lett. 427 (2006) 443–448.
[40] J.X. Guo, L. Liu, G.F. Liu, D.Z. Jia, Synthesis and solid-state photochromism of 1, 3-diphenyl-4-(2-chlorobenzal)-5-hydroxypyrazole 4-methylthiosemicarbazone, Org. Lett. 9 (2007) 3989–3992.
[41] X.Y. Xie, L. Liu, D.Z. Jia, J.X. Guo, D.L. Wu, X.L. Xie, Photo-switch and INHIBIT logic gate based on two pyrazolone thiosemicarbazone derivatives, New J. Chem. 33 (2009) 2232–2240.
[42] H. Chui, G.F. Liu, L. Liu, D.Z. Jia, Z.P. Guo, J.P. Lang, Crystal structure and spectroscopic study on photochromism of 1,3-diphenyl-4-(4′-fluoro)benzal-5-pyrazolone N(4)-phenyl semicarba-zone, J. Mol. Struct. 752 (2005) 124–129.
[43] B.S. Jensen, The synthesis of 1-phenyl-3-methtyl-4-acylpyrazolone-5, Acta Chem. Scand. 13 (1959) 1668–1670.
[44] G.M. Sheldrick, SHELXS-97 Program for the Solution of Crystal Structures, University of Göttingen, Göttingen, Germany, 1997.
[45] T. Kawato, H. Koyama, H. Kanatomi, M. Isshiki, Photoisomerization and thermoisomerization I: Unusual photochromism of *N*-(3,5-di-tert-butylsalicylidene) amines, J. Photochem. 28 (1985) 103–110.
[46] M.J. Frisch, et al., GAUSSIAN 03, Revision B. 04, Gaussian, Inc., Pittsburgh, PA, 2003.
[47] V. Sathyabama, K. Anandan, R. Kanagaraju, Quantum chemical studies of solvent effects on cytosine tautomers, J. Mol. Struct. Theochem. 897 (2009) 106–110.
[48] I. Alkorta, J. Elguero, Influence of intermolecular hydrogen bonds on the tautomerism of pyridine derivatives, J. Org. Chem. 67 (2002) 1515–1519.